Water formation on Pd(111) by reaction of oxygen with atomic and molecular hydrogen

G. Pauer and A. Winkler
Institute of Solid State Physics, Graz University of Technology, Petersgasse 16, A-8010 Graz, Austria

(Received 31 October 2003; accepted 24 November 2003)

In this work we have studied the steady-state reaction of molecular and atomic hydrogen with oxygen on a Pd(111) surface at a low total pressure ($<10^{-7}$ mbar) and at sample temperatures ranging from 100 to 1100 K. Characteristic features of the water formation rate $\Phi(p_{H_2}; p_{O_2}; T_{Pd})$ are presented and discussed, including effects that are due to the use of gas-phase atomic hydrogen for exposure. Optimum impingement ratios (OIR) for hydrogen and oxygen for water formation and their dependence on the sample temperature have been determined. The occurring shift in the OIR could be ascribed to the temperature dependence of the sticking coefficients for hydrogen (S_{H_2}) and oxygen (S_{O_2}) on Pd(111). Using gas-phase atomic hydrogen for water formation leads to an increase of the OIR, suggesting that hydrogen abstraction via hot-atom reactions competes with H_2O formation. The velocity distributions of the desorbing water molecules formed on the Pd(111) surface have been measured by time-of-flight spectroscopy under various conditions, using either gas-phase H atoms or molecular H_2 as reactants. In all cases, the desorbing water flux could be represented by a Maxwellian distribution corresponding to the surface temperature, thus giving direct evidence for a Langmuir–Hinshelwood mechanism for water formation on Pd(111). © *2004 American Institute of Physics.* [DOI: 10.1063/1.1643352]

I. INTRODUCTION

Due to its technological importance, water formation on catalytically active crystalline surfaces, such as palladium and platinum, has been studied extensively over a large pressure and temperature range, using a variety of experimental techniques. For the investigation of the reaction $H_2+O_2 \rightarrow H_2O$ on palladium under UHV conditions the applied techniques comprised coadsorption, thermal desorption spectroscopy (TDS),[1] molecular-beam relaxation[2,3] and scanning tunneling microscopy (STM).[4–6] The reactive surfaces studied were either Pd single crystals or polycrystalline palladium metal-oxide-semiconductor devices (Pd-MOS).[7–9] For studies in the high pressure regime ($1.0–10^5$ Pa), mostly Pd foils or membranes have been used.[10–13] Directly related to the water formation itself, numerous investigations also dealt with the interaction of the two single reactants hydrogen[14–18] and oxygen[19–25] with Pd surfaces, including the determination of corresponding sticking coefficients, diffusion barriers,[5,26] desorption energies and their dependence on surface temperature and coverage. It is well known that water formation is a thermally activated process with an activation barrier of 0.3–0.42 eV (Refs. 3 and 4) for OH formation on Pd(111). Due to this barrier, a minimum surface temperature of about 200 K is needed for H_2O formation. Recently, also the interaction of gas-phase hydrogen atoms with adsorbed oxygen on Pt(111) has been investigated,[27] suggesting a new reaction channel for H_2O formation at low surface temperatures (85 K) via hot atoms. In this work we have focused on differences in the kinetics of water formation on a Pd(111) single crystal surface, by using either molecular or gas-phase H atoms to react with oxygen. The experiments have been performed mostly under steady-state conditions, thus also offering the possibility of high resolution time-of-flight (TOF) measurements on desorbing H_2O, formed at the sample surface.

II. EXPERIMENTAL DETAILS

The experiments have been carried out in an ultrahigh vacuum chamber with a base pressure of 10^{-10} mbar, equipped with low energy electron diffraction (LEED), Auger electron spectroscopy (AES), a multiplexed quadrupole mass spectrometer (QMS), and an extractor ion gauge. For dosing with atomic hydrogen, a highly efficient capillary doser, designed after the concept of Bischler and Bertel[28] has been used. A detailed characterization of this doser was performed by Eibl *et al.*,[29] which allows the calculation of the number of incident atoms on the sample surface during exposure. For the water formation experiments, oxygen has always been dosed isotropically, whereas hydrogen could be dosed either isotropically (H_2) or via the atomic source (H, H_2) with a variable angle of incidence between 45°–90° and a distance of about 2.5 cm from the capillary. The UHV system also offers the possibility to measure the kinetic energy of desorbing species by a time-of-flight (TOF) unit attached to the main chamber. It consists of two differentially pumped chambers (turbomolecular-, and Ti-sublimation-pumps), the first containing a motor driven chopper-disk and the second the detector quadrupole mass spectrometer. These chambers are connected via a system of carefully aligned apertures, integrated into specifically constructed liquid nitrogen cooled cryo panels. The pressure in the TOF-detector chamber thus always stayed below 3×10^{-11} mbar, provid-

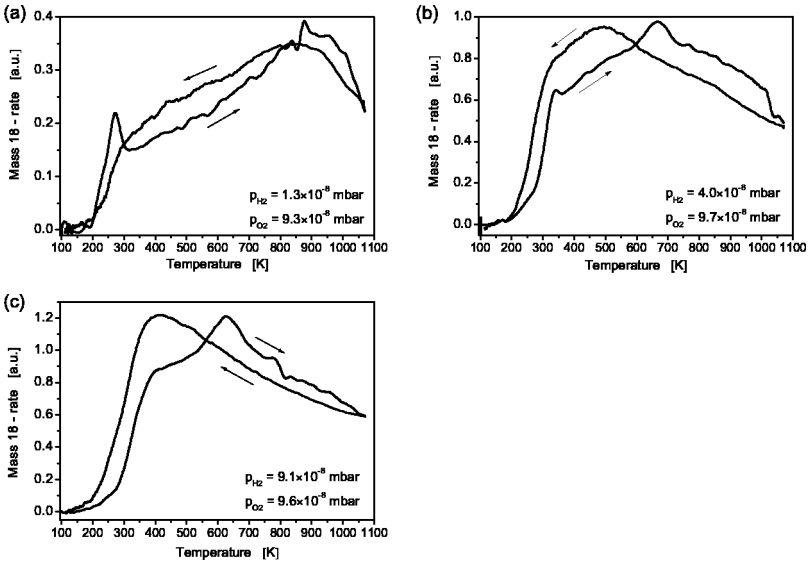

FIG. 1. Water formation rates $\Phi(p_{H_2}; p_{O_2}; T_{Pd})$ as a function of the surface temperature at fixed H_2 and O_2 partial pressures. The arrows indicate the direction of the temperature ramp ($\beta = 1$ K/s).

ing low background signal even if the total pressure in the main chamber exceeded 10^{-7} mbar. Additionally, the rather long distance of 476 mm between chopper and detector-QMS provides excellent time-resolution of the TOF spectra. For a more detailed description of the TOF unit and the evaluation of TOF spectra, see Ref. 30. The atomic doser in the main chamber is positioned at an angle of 45° with respect to the detector entrance aperture and the optical axis of the TOF unit, allowing simultaneous atomic hydrogen exposure of the sample during time-of-flight measurements. The disk shaped Pd(111) single-crystal sample (10 mm diameter) was fixed to a liquid nitrogen (LN_2) cooled sample holder by two molybdenum wires for resistive heating. The sample temperature could be varied between 97 and 1100 K. The cleanness of the sample front side was ensured by regular sputtering with Ar^+ ions at 900 K and annealing at 1100 K for about 20–30 min. To get rid of residual carbon contamination, the sample was subsequently exposed to 5×10^{-8} mbar of oxygen for about 15 min at 550 K (as proposed in Ref. 14). Finally, the sample was heated to 1100 K at 7×10^{-8} mbar hydrogen background pressure. After this treatment, thermal desorption spectroscopy (TDS) did not show any CO desorption after oxygen adsorption at 100 K. By AES surface inspection, further contamination by boron or sulfur could be ruled out, too. The rim and backside of the sample could be considered inactive, concerning hydrogen adsorption and water formation. This was evidenced by quantitative TDS of the clean Pd(111) surface, exhibiting a saturation coverage of $\sim$1.0 ML ($1\ \text{ML} = 1.53\times10^{15}$ atoms cm^{-2}) after exposure to 5–10 Langmuir of molecular hydrogen, at a sample temperature of 97 K, in accordance with Ref. 14.

III. RESULTS AND DISCUSSION

A. The $H_2+O_2\Rightarrow H_2O$ reaction on Pd(111)

The most obvious and straightforward way to analyze the reaction of hydrogen and oxygen towards water on any given surface comprises the determination of the water product rate as a function of the concentrations (i.e., coverages) of both reactants H(ad) and O(ad) at a certain temperature of the active surface. Provided that the reaction proceeds under steady-state conditions, the product rate $\Phi(\theta_{H_2}; \theta_{O_2}; T_{Pd})$ is, as a first approximation, a function of these three parameters only. As the reactant coverages (especially θ_H) were not directly observable in the steady state regime, the corresponding partial pressures p_{H_2} and p_{O_2} were used as coverage related parameters instead. Partial pressures could be continually monitored via the multiplexed quadrupole mass spectrometer. Regular calibration of the QMS detection sensitivity for hydrogen and oxygen allowed for quantitative determination of the number of H_2 and O_2 molecules actually impinging on the active surface. To allow easy subtraction of any background water contribution, the following approach has been chosen for the experimental determination of the water product rate $\Phi(p_{H_2}; p_{O_2}; T_{Pd})$: All measurements started with the clean, LN_2 cooled sample kept at $T_{Pd} = 100$ K with a background pressure in the order of 10^{-10} mbar. In the next step, constant fluxes of H_2 and O_2 were admitted into the chamber via separate leak valves. In this way, the active surface was exposed to constant isotropic gas mixtures of hydrogen and oxygen at fixed partial pressure ratios. A slow increase of the sample temperature ($\sim$1 K/s), in order to stay in a ''near steady state'' regime, finally permitted the measurement of the temperature dependent water formation on Pd(111) at a constant reactant supply with the help of the multiplexed QMS. After having reached 1100 K, the sample was cooled down again to $T_{Pd} < 110$ K. Below $\sim$200 K no OH formation (and no H_2O formation likewise) takes place on Pd(111),[4,6] so the measured water rate at the beginning and the end of each measurement (where $T_{Pd} < 110$ K) could be used to determine the H_2O background. Figures 1(a)–1(c) show exemplary H_2O-rates as a function of the surface temperature for fixed H_2 and O_2 partial pressures. Depending on the p_{H_2}/p_{O_2} ratio, these H_2O-rate curves vary significantly, concerning the temperature at maximum water production and the absolute value of the H_2O rate. Additionally, some kind of hysteresis occurs in the water formation rate between the ''heat-up''

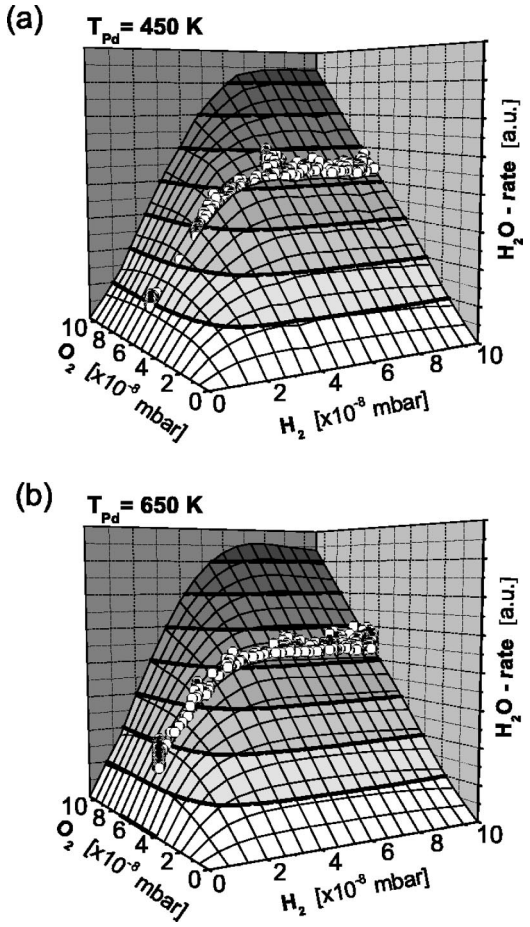

FIG. 2. Water formation rates $\Phi(p_{H_2};\ p_{O_2};\ T_{Pd})$ as a function of H_2 and O_2 pressures at fixed surface temperature (obtained from a set of measurements as shown in Fig. 1). The white circles correspond to the water formation rates obtained by varying the H_2 pressure at fixed O_2 pressure ($p_{O_2}=6.7\times10^{-8}$ mbar) and fixed sample temperatures: (a) 450 K and (b) 650 K.

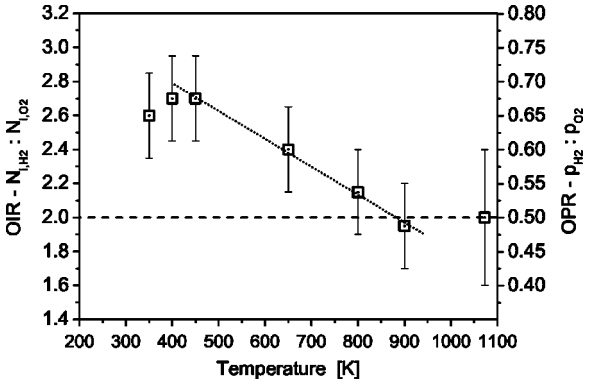

FIG. 3. Optimum impingement ratios (OIR) and optimum partial pressure ratios (OPR) for H_2O production on Pd(111) as a function of the surface temperature.

and ''cool-down'' cycles, which is partially due to the 1 K/s heating rate and a nonequilibrium initial situation resulting in desorption peaks in the heat up regime. The mean values of the water formation rates of the ''cool-down'' and ''heat-up'' cycles for a number of different H_2/O_2 ratios were used to plot the rates $\Phi(p_{H_2};\ p_{O_2};\ T_{Pd})$ in the form of three-dimensional diagrams [Figs. 2(a) and 2(b)]. The deviation of the water formation rates from the mean value are only about 10%, thus quasi-stationarity of these experiments is largely fulfilled. Two exemplary representations of the rate function $\Phi(p_{H_2};\ p_{O_2};\ T_{Pd}=\text{const.})$ for $T_{Pd}=450$ and 650 K are shown in Figs. 2(a) and 2(b). To further confirm the shapes of the rate surfaces, an alternative procedure has been applied: For fixed sample temperatures (e.g., 450 and 650 K) and a constant isotropic oxygen flux ($p_{O_2}=6.7\times10^{-8}$ mbar), the water formation rate was measured as a function of the hydrogen pressure, which was slowly varied to account for the relaxation time of water formation. Equivalent measurements at $T_{Pd}=100$ K were performed to determine the H_2/O_2-pressure dependent background H_2O-contribution. The background corrected water rate curves reproduced quite well the characteristic shapes of the rate surfaces obtained by the first method. These data are represented as white circles in the three-dimensional plots of Figs. 2(a) and 2(b). To extract some general results from these data we will first focus on the qualitative features of the reaction rates.

As the individual reactant partial pressures have been chosen within the range of 1×10^{-9}–1.3×10^{-7} mbar, which is equivalent to impingement rates of about 0.002–0.2 ML/s for hydrogen and 5×10^{-4}–5×10^{-2} ML/s for oxygen, the H and O coverages are always very small during the reaction conditions. For the applied H_2 pressures, the hydrogen coverage is very small due to rapid desorption above 300 K. By *in situ* Auger electron spectroscopy to monitor the oxygen coverage during water formation, it was found that also the oxygen signal became undetectable small a few seconds after the start of water formation, synchronous with the increase of the hydrogen flux. In Figs. 2(a) and 2(b) it is apparent, that the overall H_2O rate increases with increasing total pressure ($p_{H_2}+p_{O_2}$) for a fixed sample temperature. Therefore, the reactant supply constitutes the main rate limiting factor. On the other hand, for a given oxygen pressure, increasing the hydrogen pressure above a certain value does not lead to an equivalent increase in the H_2O rate. This bend of the $\Phi(p_{H_2};\ p_{O_2}=\text{const.};\ T_{Pd}=\text{const.})$-curve indicates the partial pressure ratio (p_{H_2}/p_{O_2}) or the impingement ratio ($N_{i,H_2}/N_{i,O_2}$), at which practically all adsorbed oxygen and hydrogen atoms are converted to H_2O. This subject will be discussed in more detail below. At this point the highest water formation rate exists for a given total pressure. We will designate this ratio the ''optimum partial pressure ratio'' (OPR), corresponding to the ''optimum impingement ratio'' (OIR) that will be used for better comparison with the experiments using gas-phase H atoms. As can be seen from the shapes of the water formation rate functions $\Phi(p_{H_2};\ p_{O_2};\ T_{Pd})$ presented in Fig. 2, the ''optimum ratios'' are independent of the total pressure in the studied pressure range ($p_{H_2+O_2}\leqslant2\times10^{-7}$ mbar). Detailed analysis of the water formation rate, for sample temperatures ranging from 300 K to 1100 K, revealed a significant temperature dependence of the OIR which is presented in Fig. 3. In the temperature range from about 300 to 500 K, the OIR shows its maximum value of $2.7\pm10\%$ (corresponding to an OPR of

about 0.67), which is followed by a linear decrease of the OIR for higher sample temperatures till a value of about $2.0 \pm 15\%$ is reached at 900 K (OPR$\approx$0.50). This value remains approximately constant up to $T_{Pd} = 1100$ K. The fact that the ''optimum ratio'' approaches the stoichiometric value (OIR$\approx$2.0) for sample temperatures above the desorption maximum of oxygen (at around 760–800 K, according to Refs. 21, 22), together with the linear decrease of the OIR in the mid temperature range suggest, that changes of the sticking coefficients of the single constituents may be the major causes for these variations.

Quantitative conclusions concerning the temperature dependent sticking coefficients can be drawn under the following assumptions: First, it is supposed that for water formation at the ''optimum ratio'' all adsorbed atoms are converted to H_2O.[8,12] Second, the sticking coefficients for both H_2 and O_2 should only depend on the sample temperature, as the total reactant coverages are small (initial sticking coefficients). This is confirmed by the fact that the water rate increases linearly with the single reactant pressure up to the point where the optimum ratio is reached. Of course, this approximation is not valid for temperatures <350 K, when H adsorption and site blocking becomes significant (coverage dependent sticking coefficient). Furthermore, any continuous loss of adsorbate, due to diffusion into the bulk, can be neglected (especially at the ''optimum pressure ratio'' [9]). An estimate of the bulk absorption rate of H_2 on the Pd(111) sample has been determined experimentally by quantitative TDS, confirming the latter statement. Other studies on Pd membranes and on Pd-MOS devices also revealed, that during water formation under comparable conditions no permeation or diffusion of hydrogen into deeper surface layers takes place.[9,12] Finally, the competing process of H_2 desorption may be neglected in a first approximation, as the water formation reaction is much faster.[7] Thus, according to the evaluation procedure given in Ref. 7, the following relationships should be valid for water formation at the ''optimum impingement ratio'' (OIR):

$$N_{\mathrm{H,ads.}} = 2 \cdot N_{\mathrm{O,ads.}}, \tag{1}$$

$$N_{i,\mathrm{H_2}} \cdot S^0_{\mathrm{H_2}}(T_{\mathrm{Pd}}) = 2 \cdot N_{i,\mathrm{O_2}} \cdot S^0_{\mathrm{O_2}}(T_{\mathrm{Pd}}) \tag{2}$$

or in another form,

$$\frac{N_{i,\mathrm{H_2}}}{N_{i,\mathrm{O_2}}} = 2 \cdot \frac{S^0_{\mathrm{O_2}}(T_{\mathrm{Pd}})}{S^0_{\mathrm{H_2}}(T_{\mathrm{Pd}})}. \tag{3}$$

By using independently determined sticking coefficients for hydrogen and oxygen, e.g., from Refs. 16, 17, 19–22 in Eq. (3), the corresponding optimum impingement ratios can be calculated and compared to the values from Fig. 3. As shown by Sjövall *et al.*,[19,20] the sticking coefficient for O_2 on Pd(111) (at translational energies corresponding to a gas at room temperature) decreases linearly with increasing sample temperature and exhibits just a weak angular dependence for sample temperatures above $T_{Pd} = 400$ K. From the data of the above mentioned references, the oxygen sticking coefficients have been estimated to be $S^0_{O_2} \approx 0.55-0.60$ at $T_{Pd} = 450$ K and $S^0_{O_2} \approx 0.45-0.50$ at $T_{Pd} = 650$ K. According to the results of Engel *et al.*,[2] the sticking coefficient of hydrogen on Pd(111) is practically independent of the sample temperature for $T_{Pd} > 400$ K. An absolute value of about $S^0_{H_2} \approx 0.45$ has been determined by Beutl *et al.*[16] Using these values, the ''optimum impingement ratios'' turn out to be $2.5 \pm 10\%$ at $T_{Pd} = 450$ K and $2.1 \pm 10\%$ at $T_{Pd} = 650$ K, respectively. These results reproduce the overall temperature dependence of Fig. 3 quite accurately, taking into account the rather large variations of sticking coefficients for H_2 on Pd(111) published in the literature.[11,16,17,19–22] In addition to that, it cannot be excluded that some contribution of the beforehand neglected H_2-desorption during water formation may be the reason for the small discrepancy between calculated and experimentally obtained OIR.

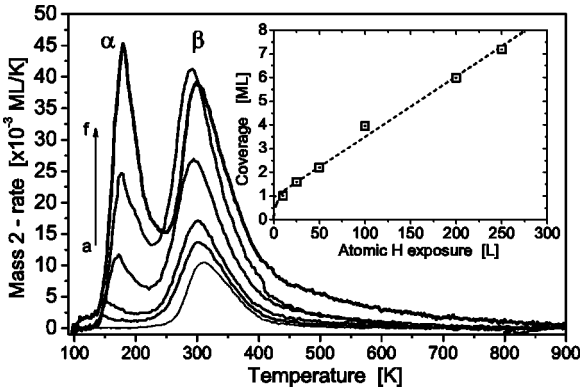

FIG. 4. Thermal desorption spectra (TDS) of H_2 after dosage of atomic H on Pd(111). Heating rate $\beta = 3$ K/s. (a) Reference spectrum - 10 L molecular H_2: 1.0 ML; (b) 25 L atomic H: 1.60 ML; (c) 50 L: 2.20 ML; (d) 100 L: 3.95 ML; (e) 200 L: 6.0 ML; (f) 250 L: 7.2 ML. The inset shows the corresponding coverage vs exposure data.

B. Atomic H exposure on Pd(111)

Before discussing the ''atomic $H + O_2$'' reaction we will present the adsorption/desorption features for pure atomic hydrogen exposure. Concerning the hydrogen desorption features and nomenclature, we refer to the work of Gdowski *et al.*,[14] who performed exhaustive TDS studies of the H_2/Pd(111) system. Similar experiments carried out on our Pd(111) single crystal with molecular hydrogen yielded comparable desorption spectra as presented in Ref. 14.

By exposure of the clean Pd(111) surface to atomic hydrogen via the hot capillary doser (2000 K) at a sample temperature of 100 K, the thermal desorption spectra presented in Fig. 4 have been obtained. In addition to the surface desorption peak (β peak) at $\sim$300 K, a rapid increase of a peak at around 170 K could be detected, which we designate as the α peak. A similar peak also shows up after extended H_2 exposure, which has been attributed to subsurface hydrogen.[14,18] Contrary to the near zeroth order shape of the α peak after dosing with molecular hydrogen, the atomic H induced peak exhibits a trailing edge towards higher desorption temperatures, which leads to a significant increase of the β peak at higher exposure. Obviously, gas-phase H atom exposure leads to a different distribution of hydrogen in the subsurface and bulk-sites thus causing the observed TDS features. Additionally, a much faster uptake of hydrogen can be

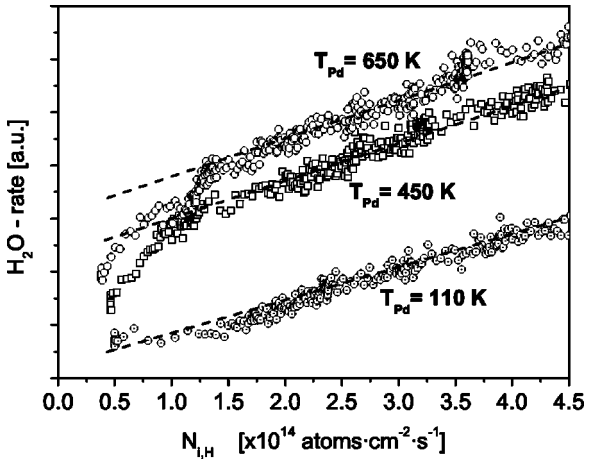

FIG. 5. H_2O-rates as function of atomic H impingement rates for different sample temperatures (at $p_{O_2}=6.7\times10^{-8}$ mbar; $N_{i,O_2}\approx3.6\times10^{13}$ atoms $\cdot\mathrm{cm}^{-2}\cdot\mathrm{s}^{-1}$).

obtained by direct impact of atomic hydrogen compared to the in-diffusion during H_2 exposure. By quantitative analysis of the TDS areas, a linear relationship between coverage and exposure could be found for exposure with atomic H (see inset of Fig. 4). The uptake rate was measured to be 0.025 ML/L*, where L* signifies the Langmuir equivalent for the number of impinging atoms during atomic H exposure ($1\ \mathrm{L}^*=2.87\times10^{15}$ H-atoms$\cdot\mathrm{cm}^{-2}\cdot\mathrm{s}^{-1}$).

C. The atomic $H+O_2\Rightarrow H_2O$ reaction on Pd(111)

For determination of the steady state water formation characteristics via the reaction of atomic H with O_2, a similar approach as described in Sec. III A has been chosen: The cleaned sample surface was exposed to a constant isotropic oxygen flux ($p_{O_2}=6.7\times10^{-8}$ mbar; $N_{i,O_2}\approx3.6\times10^{13}$ atoms$\cdot\mathrm{cm}^{-2}\cdot\mathrm{s}^{-1}$) at fixed sample temperatures, whereas the flux of atomic hydrogen, impinging at normal angle of incidence, has been slowly increased from background level to a final hydrogen pressure of $p_{H_2}\approx1.3\times10^{-7}$ mbar ($N_{i,H}\approx3.5\times10^{14}$ atoms$\cdot\mathrm{cm}^{-2}\cdot\mathrm{s}^{-1}$). The H_2O rates obtained as a function of the atomic hydrogen flux for different sample temperatures are presented in Fig. 5. The abscissa in Fig. 5 indicates the total number of impinging H atoms ($N_{i,H}$), including the directly impinging atoms from the atomic source as well as the dissociatively adsorbing hydrogen molecules from the background. As can be seen immediately, the water rate curves measured at 450 and 650 K again exhibit a characteristic bend, whereas for $T_{Pd}=110$ K only a linear increase of the water signal due to background reaction is observed. After the bend, characterizing the complete conversion of all adsorbed oxygen towards H_2O, the rates show the same linear increase as seen for the 110 K curve. Consequently, the water rate measured at $T_{Pd}=110$ K has been considered as pressure dependent H_2O background, possibly due to enhanced water formation on the copper sample holder. As the absolute water formation rates may change due to variations in pumping speed, only the ''optimum impingement ratios'' (at the bends in the H_2O rate curves) represent features that could directly be compared to the previous results of Sec. III A. Significant differences to the ''H_2+O_2'' reaction could be found for the OIR if atomic H was used [see Figs. 6(a) and 6(b)]. At a sample temperature of 450 K, the OIR for the ''atomic $H+O_2$'' reaction is measured to be $N_{i,H}/N_{i,O}=3.3\pm15\%$ (compared to the OIR of 2.7 for the ''H_2+O_2'' reaction at the same temperature) and the same value has been found for $T_{Pd}=650$ K. Thus, if gas-phase H atoms are used for water formation on Pd(111), the maximum H_2O-rates are obtained at higher hydrogen impingement ratios with no discernable dependence on the surface temperature (at least in the studied temperature and pressure range). The explanation for this surprising result is most probably the competing reaction channel of abstraction of already adsorbed hydrogen by impinging H atoms via hot-atom reactions.

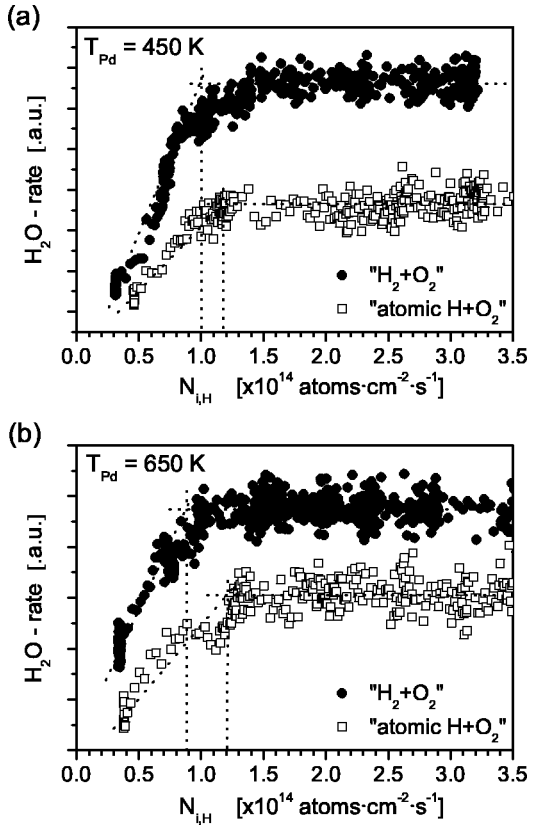

FIG. 6. Background subtracted H_2O-rates as function of atomic and molecular hydrogen flux at different sample temperatures. The constant isotropic oxygen flux was $N_{i,O_2}\approx3.6\times10^{13}$ atoms$\cdot\mathrm{cm}^{-2}\cdot\mathrm{s}^{-1}$ ($p_{O_2}=6.7\times10^{-8}$ mbar) for all experiments. Rem.: Some of the dips in the data sets are due to irregularities in the manual adjustment of a steady hydrogen partial pressure increase [e.g., at $N_{i,H}\approx1.1\times10^{14}$ atoms$\cdot\mathrm{cm}^{-2}\cdot\mathrm{s}^{-1}$ in (b)].

Similar to Sec. III A, we state that during water formation at the ''optimum impingement ratio'' a stoichiometric composition of adsorbed H and O atoms is maintained on the surface, even if abstraction of hydrogen takes place simultaneously. Therefore, a modification of Eq. (1) has to be made by taking into account the number of directly adsorbing H atoms ($N_{\text{atomic H,ads.}}$), the loss of adsorbed hydrogen via abstraction reactions ($N_{\text{H,abstract.}}$) and the contribution of dissociative adsorption of H_2 molecules from the background ($N_{\text{H,ads.}(2\pi)}$):

$$N_{\text{atomic H,ads.}} - N_{\text{H,abstract.}} + N_{\text{H,ads.}(2\pi)} = 2 \cdot N_{\text{O,ads.}}. \quad (4)$$

Additional losses of hydrogen and oxygen via further reactions, e.g. in form of direct abstraction of OH or H_2O molecules are not considered in this approximation as no experimental evidence could be found for significant occurrence of these reactions. By using the appropriate sticking coefficients (S_H, S_{H_2}, S_{O_2}) and impingements rates, as well as an abstraction coefficient (A_H) designating the probability for an impinging H atom to recombine with an already adsorbed hydrogen atom and to desorb as an H_2 molecule, Eq. (4) can be rewritten as follows:

$$N_{i,\text{atomic H}} \cdot (S_H(T_{Pd}) - A_H(T_{Pd})) + N_{i,H(2\pi)} \cdot S^0_{H_2}(T_{Pd}) = 2 \cdot N_{i,O(2\pi)} \cdot S^0_{O_2}(T_{Pd}). \quad (5)$$

It has been shown for surfaces comparable to Pd(111), e.g., for Ni(111),[31] that the initial sticking coefficient of atomic H is almost unity ($S^0_H \approx 1.0$), thus it could be stated that reflection of hydrogen atoms seems to be a rather minor effect at low coverage. From this assumption, we deduce the relation: $S_H + A_H = 1$ as a side condition to Eq. (5).

Inserting into Eq. (5) the measured total impingement rate of $N_{i,\text{H-tot.}} = N_{i,\text{atomic H}} + N_{i,H(2\pi)} \approx 1.2 \times 10^{14}$ atoms$\cdot$cm$^{-2}\cdot$s^{-1} at the bend of the H_2O formation rate signifying the OIR of 3.3, an experimentally determined ratio of $N_{i,\text{H-tot.}}/N_{i,H(2\pi)} \approx 1.7$ (depending on the doser-sample distance and the hydrogen pumping speed) and sticking coefficients as used in Sec. III A [$S_{H_2} \approx 0.45$; S_{O_2} (450 K) ≈ 0.57; S_{O_2} (650 K) ≈ 0.47], leads to the following results: At $T_{Pd} = 450$ K the abstraction probability for H atoms turns out to be $A_H = 0.40 \pm 20\%$ and the sticking coefficient $S_H = 0.60 \pm 20\%$. At $T_{Pd} = 650$ K, the corresponding values are $A_H = 0.47 \pm 20\%$ and $S_H = 0.53 \pm 20\%$. It should be noted, that an abstraction probability as defined above will generally be hydrogen coverage dependent [$A_H = f(\theta_H)$]. Therefore, the obtained values represent A_H only for the small equilibrium coverage at the OIR.

Summarizing, it can be stated that direct dosing of atomic hydrogen is rather counterproductive for water formation on Pd(111) under the studied conditions, due to the generation of hot-H-atoms which possess a high probability for hydrogen abstraction (even at low hydrogen coverages) before dissipating their excess energy. This way, the net amount of adsorbed hydrogen that is available for further reactions towards water is significantly reduced. A mechanism involving hot atoms that could possibly lead to desorption of water even at temperatures below 200 K [temperature needed to form OH from adsorbed O and H (Refs. 4, 6)], which has been found for platinum[27] or copper,[32] could not be found with the conditions used in this study.

D. TOF-measurements of generated H_2O

In Figs. 7(a) and 7(b), two examples of time-of-flight spectra for desorbing water molecules are presented (at sample temperatures of 500 K). The first spectrum was obtained by reaction of isotropic molecular H_2 and O_2 ($p_{\text{tot.}} \approx 1.7 \times 10^{-5}$ mbar; $N_{i,H_2}/N_{i,O_2} \approx 2.6$) at a gas temperature of 300 K, the second by atomic H and isotropic O_2 ($p_{\text{tot.}} \approx 4.8 \times 10^{-6}$ mbar; $N_{i,H+H_2}/N_{i,O_2} \approx 2.5$). Compared to the previous experiments, the H_2 and O_2 partial pressures for these measurements have been chosen much higher to obtain adequate water product rates for an acceptable signal to noise ratio of the TOF spectra. The detection angle was always normal to the sample surface. For H_2O formation with atomic H, a lower hydrogen flux was used to ensure a high degree of dissociation of H_2 through the hot capillary,[29] which explains the different count rates in Figs. 7(a) and 7(b). At lower sample temperatures (e.g., $T_{Pd} < 220$ K for the "atomic $H + O_2$" reaction), the resulting H_2O flux from the sample surface became too small to be detectable with our instrumentation. For evaluation of the TOF spectra a method as described in Ref. 30 has been used. In both cases of Fig. 7, the detected flux of desorbing H_2O molecules could be best described by single Maxwellian distributions corresponding closely to the temperature of the active surface (T_{Pd}). Other TOF measurements at sample temperatures of 700 K or at detection angles of 22.5° (marking the specular direction with respect to the incoming flux of hydrogen atoms) produced similar results.

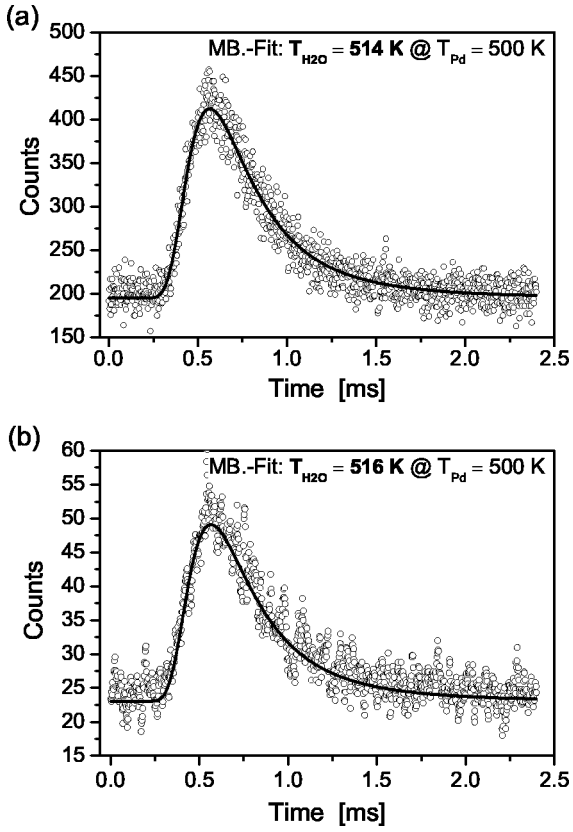

FIG. 7. Time-of-flight (TOF) spectra of H_2O molecules, formed on a Pd(111) surface at 500 K. (a) H_2O formed via molecular $H_2 + O_2$: $p_{\text{tot.}} = 1.7 \times 10^{-5}$ mbar; $N_{i,H_2}/N_{i,O_2} \approx 2.6$; (b) H_2O formed via atomic $H + O_2$; $p_{\text{tot.}} = 4.8 \times 10^{-6}$ mbar; $N_{i,H+H_2}/N_{i,O_2} \approx 2.5$; Detection angle: normal to surface. The black lines correspond to the best fits of Maxwellian TOF-distributions for H_2O to the experimental data.

Summarizing, it can be stated that water formed on a Pd(111) surface is always completely accommodated to the surface under the conditions studied. These results suggest

that hot H atoms first dissipate their excess energy before they react with adsorbed oxygen or OH to form water. An Eley–Rideal or a hot-atom-type water formation reaction, which would result in hyperthermally desorbing water molecules, could not be observed.

IV. SUMMARY AND CONCLUSION

Steady-state water formation on a Pd(111) single crystal surface has been studied at low pressures ($p_{tot}<1\times10^{-7}$ mbar) over a wide temperature range ($T_{Pd}=100-1100$ K). In the case of molecular, isotropic dosing of H_2 and O_2, a clear temperature dependence of the optimum impingement ratio for water formation was found. This temperature dependence could be ascribed to the temperature dependent sticking coefficients of H_2 and O_2 on the Pd(111) surface.

Via TDS it has been shown that dosing of atomic hydrogen, impinging at normal incidence at a sample temperature of $T_{Pd}=100$ K, leads to a fast population of subsurface states. Hydrogen in these subsurface states desorbs with a peak maximum around 170 K (α peak) and an extended slope towards higher temperatures.

The optimum impingement ratio (OIR) for water formation on a Pd(111) surface, dosing atomic H and isotropic O_2, has been found to be higher than in the case of molecular hydrogen dosing, due to hydrogen abstraction via hot-atom reactions to form H_2 competing with H_2O formation.

Time-of-flight (TOF) spectroscopy of desorbing H_2O, formed via "H_2+O_2" or "atomic $H+O_2$" reactions, revealed that the water molecules are completely accommodated to the surface for both kinds of reactions.

ACKNOWLEDGMENT

This work has been supported by the Austrian "Fonds zur Förderung der wissenschaftlichen Forschung."

[1] D. L. Weissman-Wenocur and W. E. Spicer, Surf. Sci. **133**, 499 (1983).
[2] T. Engel and H. Kuipers, Surf. Sci. **90**, 162 (1979).
[3] T. Engel and H. Kuipers, Surf. Sci. **90**, 181 (1979).
[4] T. Mitsui, M. K. Rose, E. Fomin, D. F. Ogletree, and M. Salmeron, J. Chem. Phys. **117**, 5855 (2002).
[5] T. Mitsui, M. K. Rose, E. Fomin, D. F. Ogletree, and M. Salmeron, Surf. Sci. **540**, 5 (2003).
[6] T. Mitsui, M. K. Rose, E. Fomin, D. F. Ogletree, and M. Salmeron, Surf. Sci. **511**, 259 (2002).
[7] J. Fogelberg and L.-G. Petersson, Surf. Sci. **350**, 91 (1996).
[8] H. M. Dannetun, D. Söderberg, I. Lundström, and L.-G. Peterśson, Surf. Sci. **152/153**, 559 (1985).
[9] L.-G. Petersson, H. M. Dannetun, and I. Lundström, Surf. Sci. **161**, 77 (1985).
[10] Å. Johansson, M. Försth, and A. Rosén, Int. J. Mol. Sci. **2**, 221 (2001).
[11] Å. Johansson, M. Försth, and A. Rosén, Surf. Sci. **529**, 247 (2003).
[12] M. Johansson and L.-G. Ekedahl, Appl. Surf. Sci. **173**, 122 (2001).
[13] M. Johansson and L.-G. Ekedahl, Appl. Surf. Sci. **180**, 27 (2001).
[14] G. E. Gdowski, T. E. Felter, and R. H. Stulen, Surf. Sci. **181**, L147 (1987).
[15] H. Conrad, G. Ertl, and E. E. Latta, Surf. Sci. **41**, 435 (1974).
[16] M. Beutl, M. Riedler, and K. D. Rendulic, Chem. Phys. Lett. **247**, 249 (1995).
[17] M. P. Kiskinova and G. M. Bliznakov, Surf. Sci. **123**, 61 (1982).
[18] T. E. Felter, S. M. Foiles, M. S. Daw, and R. H. Stulen, Surf. Sci. **171**, L379 (1986).
[19] P. Sjövall and P. Uvdal, J. Vac. Sci. Technol. A **16**(3), 943 (1998).
[20] P. Sjövall and P. Uvdal, Chem. Phys. Lett. **282**, 355 (1998).
[21] B. Klötzer, K. Hayek, C. Konvicka, E. Lundgren, and P. Varga, Surf. Sci. **482–485**, 237 (2001).
[22] F. P. Leisenberger, G. Koller, M. Sock, S. Surnev, M. G. Ramsey, F. P. Netzer, B. Klötzer, and K. Hayek, Surf. Sci. **445**, 380 (2000).
[23] H. Conrad, G. Ertl, J. Küppers, and E. E. Latta, Surf. Sci. **65**, 245 (1977).
[24] R. Imbihl and J. E. Demuth, Surf. Sci. **173**, 395 (1986).
[25] T. Engel, J. Chem. Phys. **69**, 373 (1978).
[26] W. Dong, V. Ledentu, Ph. Sautet, A. Eichler, and J. Hafner, Surf. Sci. **411**, 123 (1998).
[27] J. Biener, E. Lang, C. Lutterloh, and J. Küppers, J. Chem. Phys. **116**, 3063 (2002).
[28] U. Bischler and E. Bertel, J. Vac. Sci. Technol. A **11**, 458 (1993).
[29] C. Eibl, G. Lackner, and A. Winkler, J. Vac. Sci. Technol. A **16**, 2979 (1998).
[30] C. Eibl and A. Winkler, J. Chem. Phys. **117**, 834 (2002).
[31] H. Pölzl, G. Strohmeier, and A. Winkler, J. Chem. Phys. **110**, 1154 (1999).
[32] Th. Kammler and J. Küppers, J. Phys. Chem. B **105**, 8369 (2001).